

MINISTRY OF EDUCATION
AND TRAINING

VIETNAM ACADEMY OF SCIENCE
AND TECHNOLOGY

GRADUATE UNIVERSITY OF SCIENCE AND TECHNOLOGY



Nguyen Thi Minh

**STUDY ON THE FABRICATION OF A POROUS
CARRIER INTEGRATING MICROORGANISMS AND
PHOTOCATALYST PARTICLES FOR THE
TREATMENT OF SHRIMP FARMING WATER**

SUMMARY OF DISSERTATION ON BIOTECHNOLOGY

Code: 9 42 02 01

Hanoi - 2025

The dissertation is completed at: Graduate University of Science and Technology. Vietnam Academy Science and Technology

Supervisors:

1. Supervisor 1: Dr. Hoang Phuong Ha. Institute of Biology, Vietnam Academy of Science and Technology
2. Supervisor 2: Assoc.Prof. Ha Phuong Thu. Institute of Materials Science, Vietnam Academy of Science and Technology

Referee 1: Assoc.Prof. Dao Van Duong, Phenikaa School of Engineering, Phenikaa University

Referee 2: Dr. Nguyen Kim Thoa, Institute of Biology, Vietnam Academy of Science and Technology

Referee 3: Assoc.Prof. Do Khac Uan, School of Chemistry and Life sciences, Hanoi University of Science and Technology

The dissertation will be examined by Examination Board of Graduate University of Science and Technology, Vietnam Academy of Science and Technology at 14:00 p.m, on October 28, 2025.

The dissertation can be found at:

1. Graduate University of Science and Technology Library
2. National Library of Vietnam

LIST OF THE PUBLICATIONS RELATED TO THE DISSERTATION

1. **Nguyen Thi Minh**, Ha Phuong Thu, Le Thi Thu Huong, Phan Ke Son, Le Thi Nhi Cong, Mai Thi Thu Trang, Hoang Phuong Ha (2022). “*Modification of expanded clay carrier for enhancing the immobilization and nitrogen removal capacity of nitrifying and denitrifying bacteria in the aquaculture system*”. Journal of Bioscience and Bioengineering. 134(1): 41-47. DOI: 10.1016/j.jbiosc.2022.04.006.
2. Hoang Phuong Ha, **Nguyen Thi Minh**, Le Thi Nhi Cong, Phan Ke Son, Mai Thị Thu Trang, Ha Phuong Thu (2022). “*Characterization of isolated aerobic denitrifying bacteria and their potential use in the treatment of ni-trogen polluted aquaculture water*”. Current microbiology. 79(7): 209. DOI: 10.1007/s00284-022-02898-2.
3. Hoang Phuong Ha, **Nguyen Thi Minh**, Phan Ke Son, Bui Huong Giang, Le Thi Thu Huong, Chu Nhat Huy, Ho Ngoc Anh, Pham Quang Huy, Tran Xuan Khoi, Ha Phuong Thu (2024). “*Multilayer immobilizing of denitrifying *Bacillus* sp. and TiO_2 -AgNPs on floating expanded clay carrier for co-treatment of nitrite and pathogens in aquaculture water*”. RSC advances 14: 1984-1994. DOI: 10.1039/d3ra07361k.
4. **Nguyễn Thị Minh**, Hà Phương Thư, Lê Thị Thu Hương, Bùi Hương Giang, Phan Kế Sơn, Chu Nhật Huy, Mai Thị Thu Trang, Ứng Thị Diệu Thúy, Lê Thị Ánh Tuyết, Hoàng Phuong Hà (2025). “*A floatable TiO_2 -Ag photocatalyst enables effective antibiotic degradation and pathogen growth control*”. RSC advance, 15: 18324–18337. DOI: 10.1039/d5ra02333e.

I. INTRODUCTION

1. Rationale of the study

In aquaculture practices, water pollution often arises from multiple interrelated causes such as: i) high stocking density and overuse of nutrient-rich industrial feed with low feed conversion ratios, leading to the accumulation of excess organic compounds; ii) the decomposition of this organic matter produces toxic inorganic nitrogen compounds such as ammonia and nitrite; iii) the presence of these pollutants degrades water quality, creating favorable conditions for the proliferation of pathogenic bacteria; iv) the overuse of synthetic antibiotics for disease prevention and treatment results in residual antibiotics in both aquatic animals and the surrounding water. Therefore, integrated treatment solutions are urgently needed to ensure water quality and aquaculture productivity.

The photocatalyst material TiO_2 has shown great potential in treating organic pollution and effectively inhibiting pathogenic bacteria, owing to its strong oxidative properties. Under ultraviolet (UV) light ($\lambda \leq 400$ nm), TiO_2 generates reactive oxygen species (ROS), which break down complex organic compounds into water, carbon dioxide, and simple inorganic ions, thereby overcoming limitations of conventional treatment methods. These ROS also damage bacterial cells, significantly reducing pathogen density in the water. Although TiO_2 nanoparticles in powder form are highly effective for water treatment, large-scale applications are still limited due to the difficulty of separating the catalyst from water. Furthermore, TiO_2 may settle at the bottom of ponds, causing secondary pollution.

It is well known that UV light accounts for only about 5% of sunlight, while visible light ($400 \leq \lambda \leq 780$ nm) accounts for approximately 45%. To address this limitation, TiO_2 can be modified with silver nanoparticles (Ag), which are well-known for their antibacterial properties and strong light absorption in the 400–500 nm range. This modification results in the formation of $\text{TiO}_2\text{-Ag}$ nanomaterials capable of absorbing visible light and enhancing antibacterial effectiveness. To prevent sedimentation of these nanomaterials, $\text{TiO}_2\text{-Ag}$ can be immobilized onto a suitable carrier material to allow easy

recovery from the environment. While some studies have shown that TiO₂-Ag can degrade various pollutants, including ammonia and nitrite, nevertheless under the typical aquaculture pH conditions (pH 7.8–8.5) these nitrogen compounds mainly exist as NH₄⁺ and HNO₂. Due to their positive charge, they are not easily adsorbed onto the positively charged surface of TiO₂-Ag, making electrostatic repulsion a challenge. Therefore, it is necessary to combine appropriate technologies and methods to comprehensively address the inorganic nitrogen pollution in aquaculture environments.

In terms of nitrogen pollution, natural oxidation and reduction processes can be carried out by nitrifying and denitrifying bacteria. Ammonia is converted to nitrite and nitrate by ammonia-oxidizing and nitrite-oxidizing bacteria, followed by the conversion of nitrate and nitrite into nitrogen gas by denitrifying bacteria. Combining these processes enables complete nitrogen removal from polluted water. However, bacterial suspension are more likely to be washed out of the treatment system than biofilm-forming bacteria that can attach to carrier materials.

The similarity between the properties of photocatalyst materials and nitrogen-transforming bacteria suggests a promising integrated approach to address the four interrelated pollution issues mentioned above.

Recently, co-immobilization of photocatalysts and microorganisms has been proposed to enhance the degradation of certain compounds such as antibiotics and dyes. However, in our current study, we aim to address four key pollutants simultaneously: organic compounds, antibiotics, pathogenic bacteria, and inorganic nitrogen compounds in aquaculture environments. In this system, TiO₂-Ag plays the primary role in degrading organic compounds and inhibiting pathogens, while nitrogen-transforming bacteria contribute to the removal of ammonia and nitrite.

To optimize the integration of TiO₂-Ag, the carrier material should possess a large surface area and a porous structure. Additionally, its buoyant property enables effective exposure to both light and oxygen, thereby enhancing the photocatalytic performance of TiO₂-Ag. Apart from these physical characteristics, an ideal carrier for the immobilization of nitrogen-converting

bacteria should also provide essential nutrients to support bacterial growth and biofilm formation.

Based on the above considerations, this dissertation was conducted under the title: "Study on the fabrication of a porous carrier integrating microorganisms and photocatalyst particles for the treatment of shrimp farming water."

2. Research objectives:

To develop porous materials suitable for integrating nitrogen-converting bacteria and TiO₂-Ag photocatalyst particles, with the aim of creating multifunctional remediation agents capable of inhibiting pathogenic bacteria, degrading antibiotics and organic pollutants, and removing ammonia and nitrite compounds from aquaculture water.

3. Research Scope and Content:

- To fabricate expanded clay (EC) and nutrient-integrated EC materials that enhance the immobilization efficiency of TiO₂-Ag photocatalysts and nitrogen-converting bacteria on the material surface. To optimize the immobilization of TiO₂-Ag photocatalysts onto EC and evaluate the photocatalytic activity of the resulting composite material.

- To optimize the immobilization of nitrogen-converting bacteria onto EC_Alg_N and assess the nitrogen-removal efficiency of the resulting material.

- To investigate the co-immobilization of nitrite-converting bacteria onto TiO₂-Ag/EC and evaluate the effectiveness of the material in simultaneously inhibiting *V. parahaemolyticus* and removing nitrite from water.

II. DISSERTATION CONTENT

CHAPTER I: LITERATURE REVIEW

This chapter provides a comprehensive overview of environmental pollution issues associated with aquaculture practices. It analyzes the interrelated nature of organic pollution, inorganic nitrogen compounds, the emergence of pathogenic bacteria, and residual antibiotics in aquaculture environments.

It reviews and compiles scientific information on common water treatment methods used in aquaculture, highlighting the advantages of employing TiO₂-

Ag photocatalysts in the degradation of organic pollutants, antibiotic residues, and the inhibition of pathogenic bacterial growth. Furthermore, the limitations of photocatalytic processes in transforming ammonia and nitrite, thereby emphasizing the necessity of combining biological nitrification-denitrification processes with TiO₂-Ag photocatalysis to effectively address all four key pollutants in aquaculture systems.

The chapter also discusses the importance of immobilizing either TiO₂-Ag or nitrogen-converting bacteria onto carrier materials to stabilize treatment performance, facilitate material recovery and reuse and minimize secondary pollution. It compares this study with other research worldwide to clarify its novelty and provide a rationale for developing two distinct types of carrier materials, each tailored for a specific purpose: (1) A TiO₂-Ag-based photocatalytic carrier designed for the degradation of organic matter, antibiotic residues and pathogenic bacteria inhibition; (2) A bio-carrier designed to support the immobilization of nitrogen-converting bacteria for the removal of inorganic nitrogen compounds from aquaculture water.

The strengths and limitations of various carrier materials commonly applied in environmental remediation research are analyzed, along with approaches for improving their surface properties to enhance the immobilization of photocatalysts or bacteria. Based on this evaluation, expanded clay (EC), which synthesized via thermal treatment of a clay and rice husk mixture followed by rapid cooling, is selected as the carrier material. The resulting EC has a lightweight, porous structure with high surface roughness, allowing it to float on water and providing abundant anchoring sites for photocatalyst particles or nitrogen-converting bacteria.

Importantly, in addition to physical characteristics, the nutritional composition integrated onto the carrier surface should play a critical role in supporting bacterial colonization. Therefore, native EC is further modified by incorporating nano-sized nutrients (N, P, K and carbon source) to stimulate bacterial growth and enhance biofilm formation of nitrogen-converting bacteria. The resulting material is designated EC_Alg_N.

Among the various methods for immobilizing photocatalysts on solid

carriers, the sol-gel technique is identified as the most suitable for this study. The sol-gel matrix is optically transparent, allowing efficient light penetration to activate the photocatalyst, thereby ensuring high photocatalytic reaction efficiency. Moreover, sol-gel processing can be performed at low temperatures, simplifying the synthesis process and reducing energy consumption. For these reasons, the sol-gel method will be employed to immobilize TiO₂-Ag onto EC particles.

To enhance the integration of nitrogen-converting bacteria on EC_Alg_N, a combination of adsorption and cell entrapment techniques will be utilized. Bacterial cells will be dispersed in natural polymer solutions to increase their stability prior to immobilization. Thanks to the porous nature of EC, when coated with a polymeric network containing bacterial cells, the material offers abundant microenvironments for bacterial colonization and biofilm development, thereby strengthening the interaction between bacteria and the material surface.

These structural modifications to EC are expected to significantly improve its capacity to serve as a carrier for both photocatalysts and nitrogen-converting bacteria. Such advancements lay the foundation for the development of highly efficient, multifunctional treatment materials suitable for application in aquaculture water remediation.

CHAPTER 2. MATERIALS AND METHODS

2.1. MATERIALS

- Clay and rice husks were used in the synthesis of expanded clay (EC) particles. Other chemicals included TiCl₄, NaBH₄, AgNO₃, alginate, tetracycline, oxytetracycline hydrochloride, and rifampicin.

- Bacterial strains used in this study included: ammonia-oxidizing bacteria (*Nitrosomonas* sp. PD58 and *Nitrosomonas* sp. PD60) and nitrite-oxidizing bacteria (*Nitrobacter* sp. 2NM and *Nitrobacter* sp. 5NM); pathogenic bacteria: *Vibrio harveyi* VTCC 70222, *V. parahaemolyticus* VTCC 910192, and *Escherichia coli* ATCC 25922; and the probiotic strain *Lactobacillus acidophilus* LB. All strains were preserved in the microbial culture collection at the Key Laboratory of Bioprocess and Biochemical Synthesis Engineering,

Institute of Biology, VAST.

- Aquaculture water samples were collected from a white-leg shrimp (*Litopenaeus vannamei*) pond in Bac Lieu province on the 60th day of the farming cycle. These samples were used for isolating aerobic nitrite-converting bacteria.

2.2. METHODS

2.2.1. Preparation of EC and nutrient intergated-EC materials

➤ *Fabrication of expanded clay material (EC)*

EC particles were produced by pyrolyzing a mixture of clay powder (<2 mm in diameter) and ground rice husks at a 1:1 (w/w) ratio. Water was added to obtain a suitable ductility, and the mixture was molded into 1 cm diameter pellets, then air-dried to 30-40% moisture. These pellets were fired at 1200 °C for 2 hours to induce expansion. Rapid cooling was applied to preserve the porous structure of the expanded clay.

➤ *Fabrication of nutrient intergated-EC material*

Nutrients (N, P, K) in the form of (NH₄)₂SO₄, KH₂PO₄, and a carbon source - CH₃COONa were evenly dispersed in an alginate polymer solution to form nano-sized nutrient particles. Under gentle magnetic stirring, this solution was incorporated onto EC particles, resulting in the nutrient-integrated material EC_Alg_N.

2.2.2. Synthesis of TiO₂-Ag photocatalyst nanoparticles

TiO₂ nanoparticles were synthesized by precipitating TiCl₄ with ammonium hydroxide. Ag⁺ ions from 2 mM AgNO₃ (120 mL) were reduced to metallic silver using 30 mL of 9 mM NaBH₄. The resulting Ag nanoparticles were chemically deposited onto TiO₂ particles to form the TiO₂-Ag nanocomposite.

2.2.3. Immobilization of TiO₂-Ag on EC material

TiO₂-Ag suspensions were prepared with varying Ti concentrations (20.000, 25.000, 30.000 and 35.000 ppm). EC particles were added to the suspensions at a solid-to-liquid ratio of 1:2 (w/v) and shaken at 100 rpm. After 6, 12, or 18 hours of contact, the solid materials were filtered, dried at 60 °C for 5 hours, and analyzed to determine the amounts of Ti and Ag

immobilized onto the TiO₂-Ag/EC material.

2.2.4. Characterization of the fabricated materials

Surface area, pore volume, and pore diameter of EC samples were measured via N₂ adsorption-desorption isotherms at 77 K. Fourier Transform Infrared Spectroscopy (FTIR) was used to assess molecular structure. Crystalline structure was examined using a Bruker D8 Advance X-ray diffractometer, and Rietveld refinement was applied for detailed crystallographic analysis. Ti and Ag content in TiO₂-Ag materials was quantified using inductively coupled plasma mass spectrometry (ICP-MS). UV-Vis spectroscopy (UV-6300PC) was used to assess optical properties of TiO₂-Ag compared to TiO₂ and Ag alone. Dynamic light scattering (DLS) on a Malvern Zetasizer Nano ZS was used to determine nanoparticle size distribution and stability. Material morphology was analyzed via field-emission scanning electron microscopy (FESEM) and transmission electron microscopy (TEM).

2.2.5. Evaluation of the photocatalytic performance of TiO₂-Ag/EC

Photocatalytic performance tests were conducted under natural sunlight at the Institute of Biology, Vietnam Academy of Science and Technology (latitude: 21°02'57.2"N, longitude: 105°48'06.8"E), from July to September 2024, with light intensities ranging from 70–100 klux and ambient temperatures between 30–35 °C.

➤ Antibacterial activity

TiO₂-Ag/EC was tested for its ability to inactivate *V. harveyi*, *V. parahaemolyticus*, and *E. coli* (initial density ~10⁶ CFU/mL) under sunlight for 2 hours. Bactericidal efficiency was calculated as:

$$A = \log N_0 - \log N_t = \log\left(\frac{N_0}{N_t}\right)$$

where A is the bacterial removal efficiency, N₀ is the initial bacterial count, and N_t is the count after treatment.

➤ Antibiotic degradation activity

Experiments were conducted using tetracycline (TET), oxytetracycline (OTC), and rifampicin (RIF) at concentrations of 10, 20, and 30 ppm across

different pH levels (3, 5, 7, and 9). After 4 hours of solar irradiation, the degradation efficiency was calculated as:

$$\text{Removal efficiency (\%)} = \frac{C_0 - C_t}{C_0} \times 100\%$$

where C_0 and C_t are the antibiotic concentrations before and after exposure, respectively.

➤ ***COD removal activity***

- *Effect of initial COD concentration on the removal efficiency*

$\text{TiO}_2\text{-Ag/EC}$ (10% w/v) was added to solutions with varying COD concentrations (25, 50, and 100 mg/L) and exposed to sunlight for 8 hours/day (8:30 AM to 4:30 PM) to assess COD removal efficiency.

- *Effect of $\text{TiO}_2\text{-Ag/EC}$ dosage on the removal efficiency*

Various dosages (0.5%, 1%, 2.5%, 5%, and 7.5% w/v) of $\text{TiO}_2\text{-Ag/EC}$ were added to 1-liter solutions containing 100 mg/L COD. The photocatalytic degradation process was then conducted under sunlight.

2.2.6. Selection of nitrogen-converting bacteria to immobilize on nutrient-integrated EC

➤ ***Enrichment of nitrite-removal bacteria***

Water samples were enriched in BSM medium (pH ~6.5–7) for 6-7 days to isolate bacterial strains capable of removing nitrate/nitrite.

➤ ***Evaluation of nitrate/nitrite removal activity of isolated strain***

▪ *Under aerobic conditions:*

Biomass of each isolated bacterial strain was added to BSM medium containing either 20 mgN- NO_3^- /L or 20 mgN- NO_2^- /L. After 72 hours of incubation, samples were collected to determine bacterial growth and the residual nitrate/nitrite concentrations using the Griess and Salicylate methods.

▪ *Under anoxic conditions:*

To evaluate nitrate/nitrite converting under oxygen-limited conditions, experimental flasks were purged with nitrogen gas (N_2) for 15 minutes and sealed with rubber stoppers to create an anoxic environment. After 7 days of incubation, the residual concentrations of nitrate/nitrite in the medium were measured.

2.2.7. Immobilizing of nitrogen-converting bacteria onto nutrient-integrated EC material

Biomass of ammonia-oxidizing, nitrite-oxidizing, and nitrate/nitrite-converting bacteria were mixed in a 1:1:1 ratio to achieve total cell densities of approximately 10^4 , 10^5 , or 10^6 CFU/mL. Three types of carrier materials, including EC, EC_Alg, and EC_Alg_N were introduced into the bacterial suspension and statically incubated for 48-72 hours at 35 °C to promote bacterial biofilm formation and attachment. The materials were then recovered by filtration and air-dried at room temperature to obtain the bacteria-immobilized materials.

2.2.8. Evaluation of ammonia and nitrite removal efficiency of immobilized bacteria

➤ *Effect of initial ammonia and nitrite concentrations*

The bacteria-immobilized EC materials was added to experimental flasks containing 10 mL of synthetic medium with ammonia and nitrite added simultaneously at various total nitrogen concentrations (10, 30, 40, and 60 mgN/L) in a 1:1 ratio. Residual ammonia and nitrite concentrations were determined using the Phenate and Griess methods at the beginning and after 24 hours of incubation.

➤ *Evaluation of ammonia and nitrite removal in a 50-L pilot system*

Bacteria-immobilized EC_Alg_N material (1% w/v) was introduced into a 50-liter test tank containing aquaculture water collected from a whiteleg shrimp (*Litopenaeus vannamei*) pond. Ammonium ($(\text{NH}_4)_2\text{SO}_4$) and nitrite (NaNO_2) were added to reach initial total nitrogen concentrations of 40, 100, and 200 mgN/L ($\text{NH}_4^+:\text{NO}_2^- = 1:1$) in Stages I, II, and III, respectively. Changes in NH_4^+ , NO_2^- , and NO_3^- concentrations were monitored using the Phenate, Griess, and Salicylate methods, respectively.

2.2.9. Immobilizing nitrite-converting bacteria onto $\text{TiO}_2\text{-Ag}/\text{EC}$

➤ *Antibacterial effect of $\text{TiO}_2\text{-Ag}/\text{EC}$ on nitrite-converting bacteria*

Three materials, including original EC (denoted EC), EC loaded with $\text{TiO}_2\text{-Ag}$ ($\text{TiO}_2\text{-Ag}/\text{EC}$), and $\text{TiO}_2\text{-Ag}/\text{EC}$ further coated with chitosan ($(\text{TiO}_2\text{-Ag})\text{c}/\text{EC}$), were evaluated for their antibacterial activity against

the pathogenic bacterium *V. parahaemolyticus* and nitrate/nitrite-converting bacteria *Bacillus* sp. ST20 and *Bacillus* sp. ST26 at an initial density of 10^6 CFU/mL. The bacterial survival rate after treatment was calculated using the following equation:

$$\text{Survival rate (\%)} = \frac{\text{Bacterial density in sample treated by } \text{TiO}_2-\text{Ag/EC}}{\text{Bacterial density in negative control}} \times 100\%$$

➤ **Immobilization of nitrite-converting bacteria onto $\text{TiO}_2\text{-Ag/EC}$**

A bacterial suspension containing *Bacillus* sp. ST20 and ST26 (approx. 10^8 CFU/mL, mixed 1:1) was prepared and dispersed in 0.5% (w/v) sodium alginate solution for immobilization onto EC, $\text{TiO}_2\text{-Ag/EC}$, and $(\text{TiO}_2\text{-Ag})\text{c/EC}$ materials. The resulting co-immobilized materials were then evaluated for bacterial density, nitrite removal efficiency, and antibacterial activity against *V. parahaemolyticus*.

CHAPTER 3. RESULTS AND DISCUSSIONS

3.1. Fabrication of the original EC and nutrient-intergrated-EC

3.1.1. Fabrication of the original EC

The EC (Expanded Clay) material obtained after the pyrolysis process have an oval-round shape with an average weight of 1.2 ± 0.35 g (Figure 3.1). Brunauer–Emmett–Teller (BET) analysis revealed that the EC material possessed a specific surface area of 4.4 ± 0.12 m^2/g , a pore size of 25.1 ± 0.05 nm, and a pore volume of approximately 0.027 ± 0.005 cm^3/g . These characteristics are favorable for the immobilization of $\text{TiO}_2\text{-Ag}$ nanoparticles and nitrogen-converting bacteria for environmental remediation purposes.

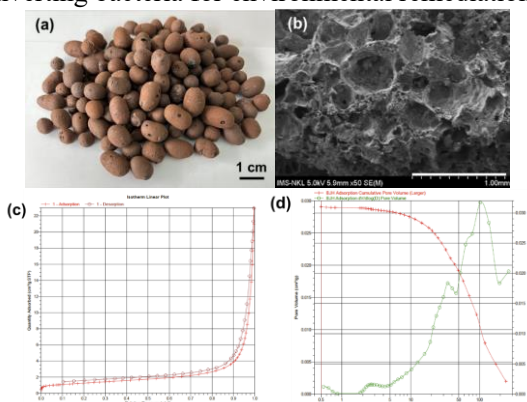


Figure 3.1. External morphology (a), internal structure (b), BET surface area plot (c), and pore size distribution (d) of the synthesized EC material.

3.1.2. Fabrication of nutrient-intergated EC

The EC material was modified by coating its surface with an alginate-based polymer containing nano-encapsulated nutrients, including ammonium sulfate ($(\text{NH}_4)_2\text{SO}_4$), carbon source - sodium acetate (CH_3COONa) and monopotassium phosphate (KH_2PO_4). This modified material (denoted as EC_Alg_N) was designed to enhance the immobilization and growth of the nitrogen-converting bacteria which are essential for the removal of ammonia and nitrite in aquaculture water. Energy-dispersive X-ray spectroscopy (EDX) analysis confirmed the successful integration of nutrient components, showing the presence of K (1.8%), N (2.28%), P (0.09%), and C (1.71%) on the surface of EC_Alg_N. In contrast, these elements were not detected on the unmodified EC material (Table 3.1), indicating that the nutrient-rich alginate layer was successfully applied.

In summary, this study successfully developed two types of functional materials: (1) EC - a porous, lightweight and floatable material suitable for the immobilization of photocatalysts ($\text{TiO}_2\text{-Ag}$) aimed at degrading organic pollutants and inhibiting pathogenic bacteria; (2) EC_Alg_N - A nutrient-enriched EC material coated with an alginate layer containing nano-sized carbon and essential nutrients (N, P, K), designed to promote microbial colonization, biofilm formation and enhanced nitrogen removal performance.

Table 3.1. Surface elemental composition of original EC and nutrient-integrated-EC (EC_Alg_N).

No.	Element	Surface elemental composition of the material	
		Original EC (EC)	Nutrient integrated - EC (EC_Alg_N)
1	O	57.43%	41.58%
2	Al	14.31%	11.56%
3	Si	13.54%	12.88%
4	Fe	11.92%	26.91%
5	K	1.52%	1.80%

6	Mg	0.89%	0.61%
7	C	-	1.71%
8	N	-	2.28%
9	S	-	0.18%
10	Ca	-	0.39%
11	Ag	-	0.01%
12	P	-	0.09%
13	Ti	0.39%	-
Total		100%	100%

3.2. Immobilization of TiO₂-Ag onto EC and evaluation of its material properties

3.2.1. Synthesis of the TiO₂-Ag photocatalyst nanoparticles

TiO₂-Ag nanoparticles were synthesized via a chemical reduction method, in which silver nanoparticles were deposited onto the surface of TiO₂ particles. The AgNPs exhibited an average size of 25.29 ± 3.61 nm, and were clearly observable on the surface of larger TiO₂ particles, which measured approximately 98 ± 11 nm in diameter (Figure 3.2, Table 3.2). FTIR and X-ray diffraction analyses confirmed the stable presence of Ag within the TiO₂ matrix without disrupting the crystal structure of TiO₂. The TiO₂-Ag nanocomposite also demonstrated excellent colloidal stability when dispersed in alginate polymer, with a zeta potential of -43.70 ± 1.12 mV (Figure 3.3, Table 3.2). Furthermore, UV-Vis spectroscopy (Figure 3.3c) revealed that Ag modification introduced surface plasmon resonance (SPR) effects, shifting the absorption edge of TiO₂ from 460 nm to the 700-800 nm range within the visible light region. This modification effectively reduced the bandgap energy of the TiO₂-Ag nanocomposite to 2.0 eV, enhancing its photocatalytic performance under visible light.

Table 3.2. Size distribution, zeta potential and concentration of the TiO₂, Ag and TiO₂-Ag contents in the composite.

	Size distribution (nm)	Zeta potential (mV)	Concentration (ppm)
TiO ₂	97.75 ± 11.06	-47.2 ± 6.42	4976.82 ± 45.20

Ag	25.29 ± 3.61	-35.51 ± 13.10	185.49 ± 14.63
TiO ₂ -Ag	458.90 ± 18.51	-43.70 ± 1.12	Ti: 4852.51 ± 23.72
			Ag: 194.58 ± 6.29

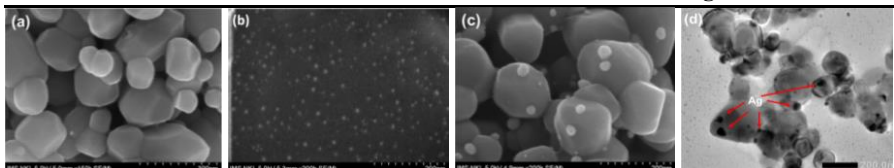


Figure 3.2. FESEM, TEM images of TiO₂ (a), Ag (b), TiO₂-Ag (c), TiO₂-Ag

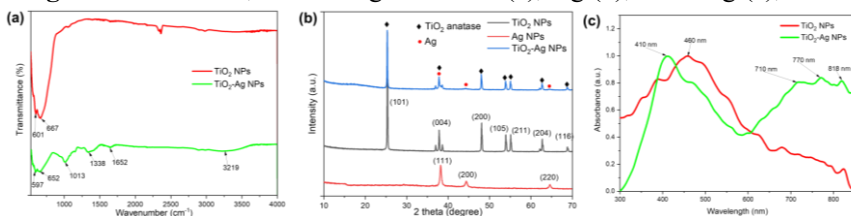


Figure 3.3. FTIR (a), X-ray diffraction (b) and UV–Vis (c) specctrums of the photocatalyst materials.

3.2.2. Optimizing the immobilization of TiO₂-Ag onto EC material

The TiO₂-Ag nanoparticles were immobilized onto expanded clay (EC) by dispersing the photocatalyst into an alginate matrix and incorporating this composite onto the EC material under continuous stirring. The alginate chains, loaded with TiO₂-Ag nanoparticles, wrapped around the EC particles (Figure 3.4), while the porous structure of EC provided numerous anchoring sites for effective attachment..

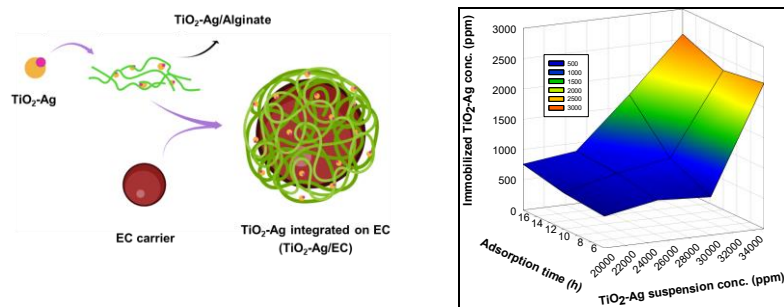


Figure 3.4. Effect of immobilization time and TiO₂-Ag suspension concentrations used on the immobilization efficiency.

The immobilization efficiency was found to be influenced by both the physicochemical properties and concentration of $\text{TiO}_2\text{-Ag}$, as well as the structural characteristics of the EC material itself. Among tested conditions, a $\text{TiO}_2\text{-Ag}$ concentration of 35.000 ppm and an immobilization time of 12 hours were optimal, yielding the highest titanium content on EC, exceeding 2.500 ppm.

3.2.3. Evaluation of the photocatalytic activity of $\text{TiO}_2\text{-Ag/EC}$

➤ Antibacterial activity against pathogens

The photocatalytic activity of $\text{TiO}_2\text{-Ag}$ activated under sunlight effectively suppressed bacterial growth, rapidly reducing bacterial densities from 10^6 CFU/mL to 7, 68, and 12 CFU/mL for *V. harveyi*, *V. parahaemolyticus*, and *E. coli*, respectively. These reductions correspond to antibacterial efficiencies of 6.0, 5.1, and 5.8 Log (N_0/N_t) (Figure 3.5).

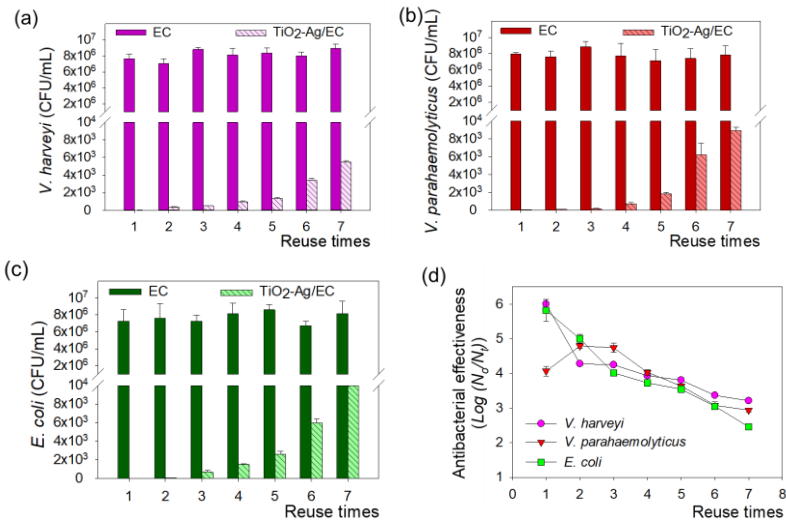


Figure 3.5. Inhibitory effect of the $\text{TiO}_2\text{-Ag/EC}$ against *V. harveyi* (a), *V. parahaemolyticus* (b), *E. coli* (c) and their corresponding bacterial inactivation efficiencies (d).

After the seven reuse times, the antibacterial performance gradually declined from 5.1–6.0 Log (N_0/N_t) to 2.5–3.2 Log (N_0/N_t). However, the material still reduced the bacterial load from 10^6 CFU/mL to approximately 10^3

CFU/mL after 2 hours of exposure, even on the seventh reuse. This suggests that $\text{TiO}_2\text{-Ag/EC}$ remains an effective material for rapid pathogen elimination in aquaculture environments.

➤ Antibiotic degradation capacity

The $\text{TiO}_2\text{-Ag/EC}$ material demonstrated strong degradation performance against the antibiotics tetracycline (TET), oxytetracycline (OTC), and rifampicin (RIF), with removal efficiencies varying depending on initial antibiotic concentration and solution pH.

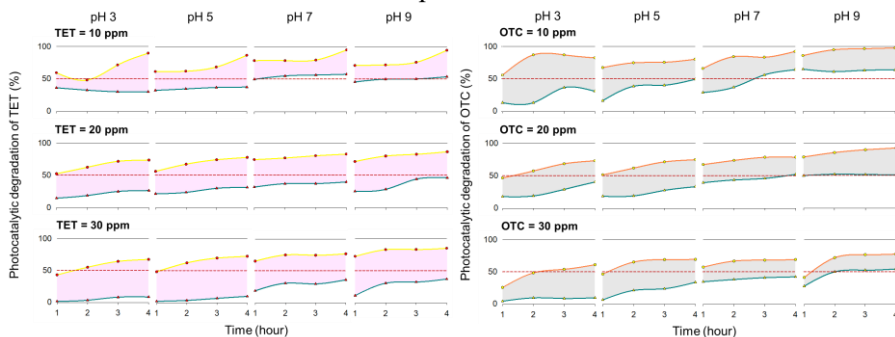


Figure 3.6. Photodegradation efficiency of TET (left) and OTC (right) by $\text{TiO}_2\text{-Ag/EC}$ material.

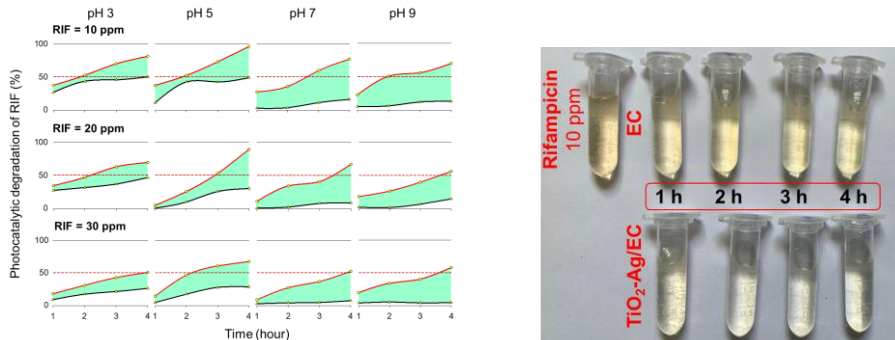


Figure 3.7. Photodegradation efficiency of RIF by $\text{TiO}_2\text{-Ag/EC}$ material.

At an initial concentration of 10 ppm, $\text{TiO}_2\text{-Ag/EC}$ removed over 92% of both TET and OTC after 4 hours of sunlight exposure at pH 7-9. RIF (10 ppm) was most effectively degraded at pH 5, with a maximum efficiency of 95.7%. Under sunlight alone, antibiotics underwent partial transformation via direct

photolysis, but this was significantly less efficient compared to the photocatalytic degradation facilitated by $\text{TiO}_2\text{-Ag/EC}$ (Figures 3.6, 3.7).

➤ **COD removal efficiency**

As shown in Figure 3.8, under sunlight irradiation, the $\text{TiO}_2\text{-Ag/EC}$ composite removed $92.9 \pm 0.7\%$ of an initial COD concentration of 25 mg/L after 32 hours. Increasing the initial COD concentration to 50 or 100 mg/L did not significantly impact performance, with removal efficiencies remaining above 86% after 40 hours.

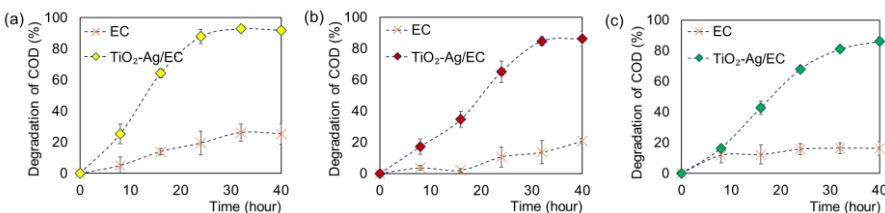


Figure 3.8. Dependence of the COD removal activity of $\text{TiO}_2\text{-Ag/EC}$ on initial COD concentrations: 25 mg/L (a), 50 mg/L (b), and 100 mg/L (c).

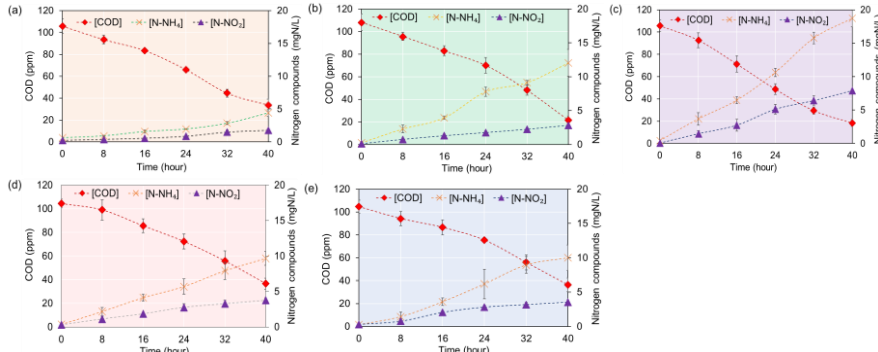


Figure 3.9. Effects of various concentrations of $\text{TiO}_2\text{-Ag/EC}$ additions: 0.5% (a), 1% (b), 2.5% (c), 5% (d) and 7.5% (e) w/v on COD removal efficiency.

To evaluate the effect of varying photocatalyst loading on COD treatment efficiency. $\text{TiO}_2\text{-Ag}$ was added at different concentrations (0.5, 1, 2.5, 5, and 7.5% w/v) to a 1-liter treatment system with an initial COD of 100 mg/L (Figure 3.9). The optimal performance was observed at a loading of 2.5% w/v, achieving a COD removal efficiency of $82.7 \pm 2.0\%$ after 40 hours of sunlight exposure. Further increases in photocatalyst dosage did not enhance efficiency,

likely due to the fixed surface area and volume of the treatment system. It is recommended that this photocatalytic method be combined with biological treatment to concurrently remove secondary pollutants such as NH_4^+ and NO_2^- , which may form during the photocatalytic degradation of organic compounds.

3.3. Immobilization of nitrogen-converting bacteria onto EC_Alg_N

3.3.1. Selection of aerobic nitrite-removing Bacteria

Water samples collected from the farming pond of white-leg shrimp (*Litopenaeus vannamei*) were used to isolate two bacterial strains, *Bacillus* sp. ST20 and *Bacillus* sp. ST26, which exhibited superior nitrate/nitrite removal efficiency under aerobic conditions. Their removal rates reached 95.2% and 97.0%, respectively, significantly higher than those observed under anaerobic conditions (Figure 3.10). These findings indicate that strains ST20 and ST26 are suitable for application in various treatment systems, especially in aquaculture ponds where continuous aeration is required for livestock survival.

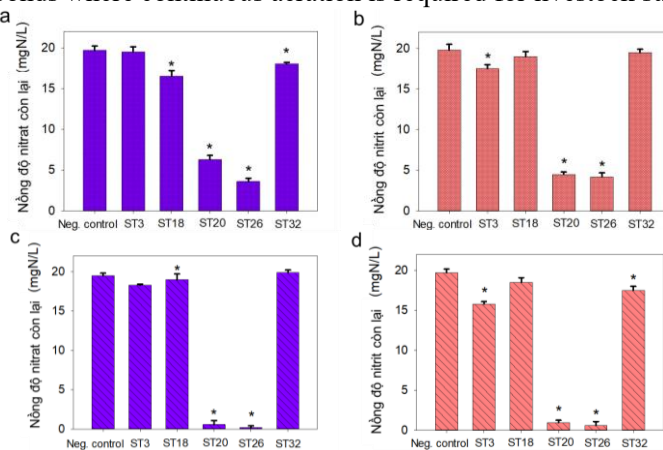


Figure 3.10. Denitrification activity of isolated strains under different conditions. **a, b** In anoxic, NO_3^- and NO_2^- as N-source, respectively. **c, d** In oxic, NO_3^- and NO_2^- as N-source, respectively.

3.3.2. Selection of the nitrifying bacteria

Results presented in Figure 3.11 demonstrate that strains ST20 and ST26 do not exhibit antagonistic growth interactions with ammonia-oxidizing bacteria (PD58, PD60) or nitrite-oxidizing bacteria (2NM, 5NM). In addition,

Table 3.3 reveals that all six selected strains were capable of forming biofilms, as evidenced by the gradual increase in OD₅₇₀ values over time, reaching a maximum after four days of cultivation. These strains were subsequently co-cultured in further experiments to evaluate the efficiency of simultaneous ammonia and nitrite – removing activity in aquaculture environments.

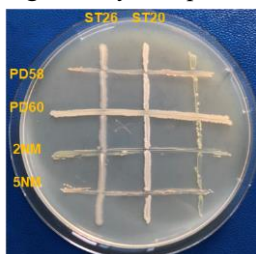


Figure 3.11. Coexistence of nitrifying and denitrifying bacteria

Table 3.3. Biofilm-forming ability of the bacteria

Strain	OD ₅₇₀				
		1 st day	2 nd day	3 rd day	4 th day
Ammonia oxidizing bacteria	PD 58	0.12 ± 0.03	0.15 ± 0.01	0.32 ± 0.05	0.41 ± 0.01
	PD 60	0.09 ± 0.03	0.18 ± 0.05	0.23 ± 0.01	0.30 ± 0.09
Nitrite oxidizing bacteria	2NM	0.07 ± 0.04	0.10 ± 0.02	0.19 ± 0.01	0.25 ± 0.02
	5NM	0.14 ± 0.01	0.14 ± 0.02	0.16 ± 0.03	0.29 ± 0.04
Nitrate/nitrite converting bacteria	ST20	0.58 ± 0.06	0.49 ± 0.01	0.54 ± 0.08	0.89 ± 0.16
	ST26	0.27 ± 0.02	0.29 ± 0.08	0.36 ± 0.07	0.33 ± 0.13

3.3.3. Optimization of bacterial immobilization on EC_Alg_N

The nutrient-integrated EC_Alg_N material contains essential nutrient such as N, P, K, carbon source and trace elements-provides a favorable microenvironment for the biofilm formation of nitrifying and nitrate/nitrite removing bacteria. As shown in Table 3.4, the optimal initial bacterial concentration for immobilization was 10⁵ CFU/mL. After two days of incubation, the immobilized bacterial populations reached (69 ± 1) × 10⁷, (57 ± 3) × 10⁷, and (430 ± 30) × 10⁷ CFU/g for ammonium-oxidizing, nitrite-oxidizing, and nitrate/nitrite-removing bacteria, respectively.

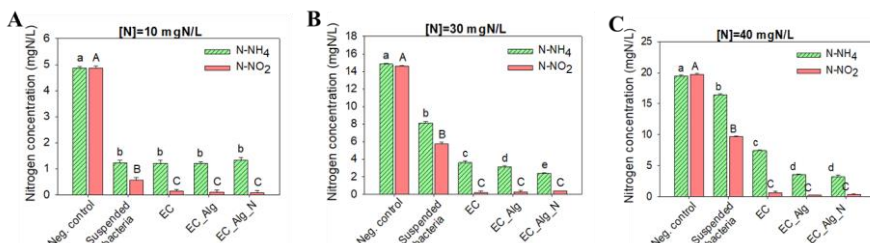
Table 3.4. Effect of the initial bacterial suspension density and material types on the immobilization efficiency.

Initial bacterial suspension density	Immobilization time	Material types	Density of immobilized bacteria (x 10 ⁷ CFU/g EC)		
			Ammonia oxidizing bacteria	Nitrite oxidizing bacteria	Nitrate/nitrite converting bacteria
10 ⁴ CFU/mL	2 nd day	EC	1.2 ± 0.2	1.4 ± 0.7	5.5 ± 3.9
		EC_Alg	1.5 ± 0.9	4.3 ± 0.9	87 ± 24
		EC_Alg_N	1.3 ± 0.4	18.1 ± 2.6	93 ± 3.3
	4 th day	EC	2.6 ± 0.3	5.8 ± 3	11 ± 5.0
		EC_Alg	2.8 ± 0.4	23.2 ± 9.5	162.8 ± 1.2
		EC_Alg_N	3.3 ± 0.5	39 ± 4.0	294 ± 28
10 ⁵ CFU/mL	2 nd day	EC	5.6 ± 0.6	3.2 ± 0.5	19 ± 9
		EC_Alg	3.3 ± 0.3 ^a	45 ± 2 ^a	210 ± 60 ^a
		EC_Alg_N	69 ± 1 ^b	57 ± 3 ^b	430 ± 30 ^b
	4 th day	EC	6.1 ± 1.1	2.8 ± 1	35 ± 12
		EC_Alg	4.0 ± 0.5	20 ± 1	230 ± 32
		EC_Alg_N	58 ± 13	46 ± 6.5	419 ± 28
10 ⁶ CFU/mL	2 nd day	EC	4.3 ± 0.27	5 ± 0.6	26 ± 9
		EC_Alg	4.9 ± 3.1 ^a	39 ± 12	183 ± 10
		EC_Alg_N	34 ± 8	63 ± 19	425 ± 83
	4 th day	EC	2.1 ± 0.3	3.9 ± 0.7	22 ± 3.5
		EC_Alg	5.8 ± 2.2	38 ± 0.8	149 ± 53
		EC_Alg_N	15 ± 9.2	50 ± 7.4	402 ± 74

3.3.4. Nitrogen removal efficiency of the bacterial immobilized EC_Alg_N

➤ Effect of initial ammonium and nitrite concentrations

As shown in Figure 3.14. the EC_Alg_N material exhibited high removal efficiencies for ammonium and nitrite (>91.62 ± 0.67%) when the initial nitrogen concentration was as high as 60 mg-N/L. This performance surpassed that of free bacterial cells or bacteria immobilized on unmodified EC. Furthermore, EC_Alg_N showed excellent reusability, maintaining a nitrogen removal efficiency of 83.95 ± 0.15% after six treatment cycles.



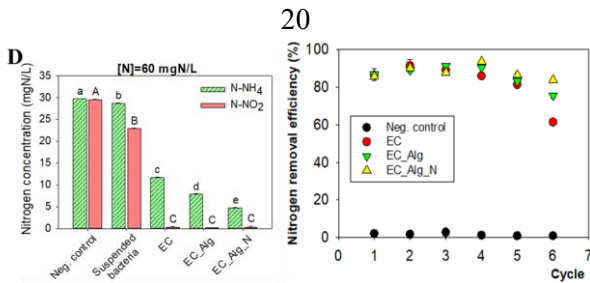


Figure 3.14. Nitrogen removal by bacteria immobilized EC at different concentration of 10 mg-N/L (a), 30 mg-N/L (b), 40 mg-N/L (c), and 60 mg-N/L (d). Reusability of the bacterial-immobilized material (e).

➤ **Nitrogen removal in a 50-Liter pilot-scale system**

To evaluate its long-term stability, EC_Alg_N with immobilized bacteria was tested in a 50-liter treatment system. When applied at a dosage of 1% w/v, the material consistently achieved >96% simultaneous ammonia and nitrite removal efficiency, even as the total nitrogen load increased from 40 to 200 mg-N/L over a 21-day period (Figure 3.15).

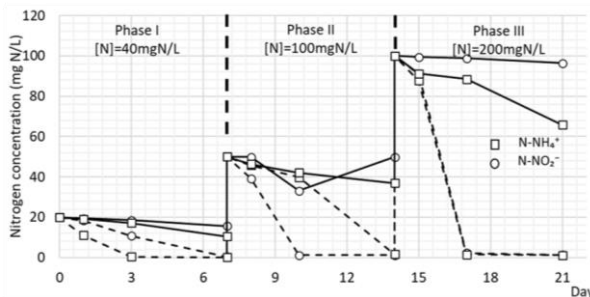


Figure 3.15. The changing of nitrogen content in the suspended cell-added bioreactor (solid line) and immobilized bacteria-added bioreactor (dash line),

$$[N] = [N\text{-NH}_4^+] + [N\text{-NO}_2^-].$$

3.4. Co-immobilization of nitrite-removing bacteria onto TiO₂-Ag/EC

In aquaculture systems, elevated nitrite levels not only impair oxygen transport in aquatic organisms and disrupt endocrine functions, but also promote the proliferation of pathogenic bacteria, particularly *Vibrio* spp., which cause acute hepatopancreatic necrosis disease. Therefore, creating a safe aquaculture environment requires the combined application of inorganic nitrogen removal and pathogen suppression strategies. In this context, our study

aims to co-immobilize nitrite-converting bacteria on $\text{TiO}_2\text{-Ag/EC}$ material to develop a multifunctional material capable of both pathogen inhibition and nitrite transformation.

3.4.1. Effect of $\text{TiO}_2\text{-Ag/EC}$ on nitrite-converting bacteria

As shown in Figure 3.16, the $(\text{TiO}_2\text{-Ag})_c/\text{EC}$ material exhibited strong antibacterial activity, inhibiting *V. parahaemolyticus* by up to $99.93 \pm 0.1\%$. However, under similar experimental conditions, the survival rates of denitrifying bacteria *Bacillus* sp. ST20 and ST26 were not significantly affected, maintaining viability rates of $95.70 \pm 3.26\%$ and $12.60 \pm 8.22\%$, respectively.

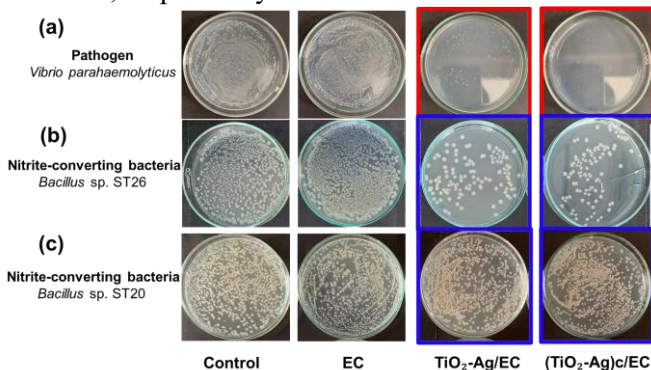


Figure 3.16. Differential of antibacterial activity of the synthesized photocatalytic agents against *V. parahaemolyticus* pathogen (a), nitrate/nitrite-converting *Bacillus* sp. ST20 (b) and *Bacillus* sp. ST26 (c).

3.4.2. Co-immobilization of nitrite-converting bacteria on $\text{TiO}_2\text{-Ag/EC}$

To enhance bacterial immobilization efficiency and minimize the detrimental effects of ROS generated by $\text{TiO}_2\text{-Ag}$, cells of the two selected nitrite-converting *Bacillus* strains were encapsulated within an alginate polymer prior to their integration onto the $(\text{TiO}_2\text{-Ag})_c/\text{EC}$ material. Chitosan and alginate are two naturally polymers with opposite surface charges. By leveraging this electrostatic property, the bacterial biomass encapsulated in alginate can be efficiently immobilized onto $(\text{TiO}_2\text{-Ag})_c/\text{EC}$, whose surface is coated with chitosan, through electrostatic attraction. The immobilization process was carried out over a 4-day period for three materials: EC, $\text{TiO}_2\text{-}$

Ag/EC, and (TiO₂-Ag)c/EC. As shown in Figure 3.17, on Day 4, (TiO₂-Ag)c/EC achieved the highest bacterial density at $(76.67 \pm 9.43) \times 10^7$ CFU/g, which was significantly higher than that of TiO₂-Ag/EC ($(33.33 \pm 4.71) \times 10^7$ CFU/g) and EC alone (5.0×10^7 CFU/g). The co-immobilized (TiO₂-Ag)c/EC material also exhibited a nitrite removal efficiency of 95.5%, which was notably higher than that of EC without modification. Furthermore, as illustrated in Figure 3.18, the integration of nitrite-converting bacteria did not compromise the photocatalytic antibacterial activity of the material against *V. parahaemolyticus*.

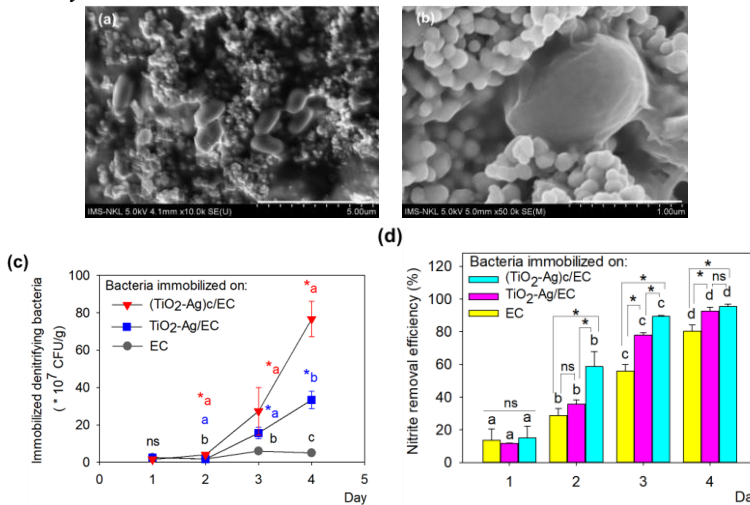


Figure 3.17. FESEM images (a and b) of the denitrifying bacteria immobilized on (TiO₂-Ag)c/EC material; bacteria density (c) and nitrite removal efficiency (d) of bacteria immobilized on various materials at different times.

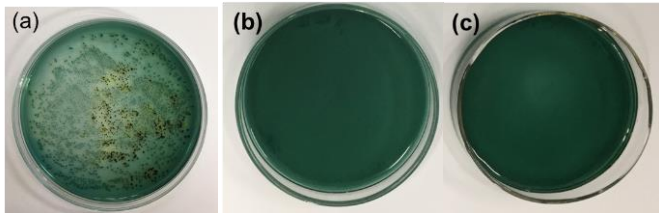


Figure 3.18. Anti-*V. parahaemolyticus* activity of TiO₂-Ag/EC (b) and bacterial-immobilized TiO₂-Ag/EC materials (c). The negative control sample was tested without any material added (a).

CONCLUSION

1. Successful fabrication of EC (Expanded Clay) material from a mixture of clay and rice husk via pyrolysis, resulting in a lightweight, porous structure with high surface roughness, buoyant on water, and suitable for the integration of photocatalysts and nitrogen-converting bacteria. The ability to float of EC facilitates effective exposure to light and oxygen, thereby enhancing treatment efficiency in aquaculture water environments.

2. Optimized integration of $\text{TiO}_2\text{-Ag}$ onto EC yielded a floating photocatalytic material with high treatment efficiency. At a dosage of 10% (w/v) $\text{TiO}_2\text{-Ag}/\text{EC}$, the material exhibited strong antibacterial activity, reducing the density of pathogenic bacteria from 10^6 to below 100 CFU/mL after 2 h of sunlight irritation, while maintaining stable performance over at least seven reuse cycles. $\text{TiO}_2\text{-Ag}/\text{EC}$ also achieved >90% degradation of tetracycline (TET) and oxytetracycline (OTC) (10 ppm) at pH 7–9, and 95% degradation of rifampicin (RIF) at pH 5; simultaneously achieving >92% COD removal (25 mg/L) after 32 h of illumination, and retaining 83% COD removal efficiency in a 1 L model with only 2.5% (w/v) dosage.

3. Notably, nitrate/nitrite-reducing bacteria were successfully isolated under aerobic conditions, enhancing nitrogen removal efficiency in oxygen-rich aquaculture environments.

4. Modification of EC by coating with an alginate polymer layer containing nano-sized nutrients (N, P, K and a carbon source) stimulated the growth and biofilm formation of aerobic nitrifying and nitrate/nitrite-reducing bacteria on the material surface. After two days of cultivation, the density of integrated aerobic nitrifying and nitrate/nitrite-reducing bacteria on the modified EC (EC_Alg_N) increased from 10^5 to 10^7 CFU/mL. At a dosage of 10% (w/v), EC_Alg_N removed 91% of ammonia and nitrite at a concentration of 60 mg N/L within 24 h, and maintained 83% removal efficiency after six reuse cycles. In a 50 L bioreactor, a dosage of only 1% (w/v) EC_Alg_N removed >96% of ammonia and nitrite when the total nitrogen concentration reached 200 mg N/L after seven days of operation.

5. Successful integration of EC loaded with $\text{TiO}_2\text{-Ag}$ photocatalyst and

aerobic nitrite-reducing bacteria produced a composite material capable of inhibiting *Vibrio parahaemolyticus* VTCC 910192 and removing up to 95% of nitrite nitrogen from contaminated water.

NEW CONTRIBUTIONS OF THE THESIS

1. Expanded clay (EC) material were fabricated from clay and rice husk components via pyrolysis. The resulting EC exhibited light weight, porous structure, and high surface roughness, making them suitable for the successful integration of TiO₂-Ag photocatalysts and nitrogen-converting bacteria. The ability to float of EC on the water surface facilitates exposure to light and oxygen, thereby enhancing photocatalytic performance. Modification of TiO₂ with Ag nanoparticles shifted the absorption wavelength range from 460 nm to 700–800 nm, resulting in increased antibacterial efficiency (reducing bacterial density from 10⁶ to <10² CFU/mL after 2 h of sunlight irradiation), COD removal (83–92%), and degradation of over 90% of residual antibiotics in aquaculture water.

2. The EC material was further integrated with nano-sized nutrients (N, P, K and a carbon source), which promoted the growth, biofilm formation, and adhesion of nitrifying and denitrifying bacteria on the material surface. Notably, nitrate/nitrite-reducing bacteria were successfully isolated under aerobic conditions, which is advantageous for nitrogen removal in aquaculture environments with high dissolved oxygen concentrations.

3. The successful co-immobilization of TiO₂-Ag photocatalyst and nitrite-reducing bacteria onto EC resulted in a composite material capable of inhibiting the pathogenic bacterium *Vibrio parahaemolyticus* VTCC 910192 and removing up to 95% of nitrite pollutants from water.